Chemical Science

ROYAL SOCIETY OF CHEMISTRY

EDGE ARTICLE

View Article Online
View Journal | View Issue

Cite this: *Chem. Sci.*, 2026, **17**, 8189

All publication charges for this article have been paid for by the Royal Society of Chemistry

Received 19th January 2026
Accepted 20th February 2026

DOI: 10.1039/d6sc00526h

rsc.li/chemical-science

N–H/P–H bond activation of ammonia, amines and phosphines at a transient borylene

Marco Weber,†[ab] Sourav Kar,†[ab] Pia Joos,[ab] Rian D. Dewhurst[ab] and Holger Braunschweig *[ab]

The metal-free activation of amines and phosphines is of great significance due to its broad relevance in both organic synthesis and industrial chemistry. Herein, we report the cooperative 1,2-addition of N–H bonds from ammonia as well as various primary and secondary amines, and the 1,1-addition of P–H bonds from primary phosphines, across the C=B double bond of a transient cyclic (alkyl)(amino)carbene (CAAC)-stabilized arylborylene. This transient borylene species displays remarkable ambiphilicity, enabling selective, metal-free activation of amines and phosphines. Mechanistic studies reveal distinct activation pathways dictated by the electronic and steric properties of the substrates, highlighting the unique reactivity of CAAC-stabilized borylenes.

Introduction

Amines and phosphines are the foremost classes of compounds of group 15 due to their extensive use as sources of nitrogen and phosphorus for organic synthesis. In particular, the rising global demand for N-containing compounds in the fertilizer, pharmaceutical, food, fuel, cement, paint, and textiles industries augmented the necessity to develop a system for activating various amines.[1–5] However, amine activation remains challenging due to the high energy required to break the N–H bond.[6] As a result, most transition metals tend to form Werner-type complexes with amines rather than undergo direct N–H bond activation.[7] Nevertheless, a substantial number of examples of transition metal-assisted amine N–H bond activation have been reported, proceeding *via* oxidative addition,[8–10] metal–ligand cooperativity,[11–14] deprotonation,[15,16] and bimetallic addition.[17] Notably, both catalytic hydroamination and the Buchwald–Hartwig amination involve N–H activation as a key step in their respective C–N bond formation catalytic cycles, enabled by transition metals.[18–24]

Bertrand's cyclic (alkyl)(amino)carbenes (CAACs) have provided an alternative platform to overcome the limitations associated with transition-metal-mediated amine activation.[25] Similar to transition metals, these species exhibit ambiphilic character arising from a filled nonbonding orbital and an accessible vacant p orbital. These electronic features enabled the metal-free oxidative addition of ammonia to the carbene carbon center. Following this discovery, a variety of low-valent group 13–15 species have also been employed for ammonia activation, such as stannylenes, gallylenes, silylenes, disilenes, and complexes based on phosphorus(III) or (I).[26–38]

The boron analogs of carbenes, free borylenes, of the form [:BR], possess vacant p-orbitals and a lone pair of nonbonding electrons, are highly reactive and have short lifetimes.[39–44] Direct spectroscopic observation of organoborylenes, [:BR], is extremely rare and has only been achieved in matrix-isolation studies.[45–47] In 1984, Pachaly and West reported the pronounced ambiphilicity and reactivity of an *in situ*-generated borylene, [:B(SiPh$_3$)], in C–H and C≡C activation reactions (Fig. 1A).[48] However, due to the synthetic challenges, progress in metal-free borylenes remained limited until the isolation of the doubly base-stabilized borylene [(^{Cy}CAAC)$_2$BH] (^{Cy}CAAC = 2-(2,6-diisopropylphenyl)-3,3-dimethyl-2-azaspiro[4,5]decan-1-ylidene), by Bertrand and coworkers in 2011.[49] Subsequently, the same group reported the singly base-stabilized dicoordinate borylene, [(Me$_3$Si)$_2$NB(^{Cy}CAAC)], which was shown to activate H$_2$ and CO (Fig. 1B).[50] Recently, we employed transient dicoordinate borylene species of the form [(CAAC)BAr] in the activation (Fig. 1C)[51] and reductive coupling of N$_2$.[52,53] The resulting bis(borylene)–dinitrogen complex was further shown to provide access to a number of N-heterocycles as well as ammonium chloride.[54,55] Mo and Wang recently reported the bis(silylene)-stabilized-borylene-mediated cleavage of the N–H bond in aniline, in which the hydrogen atom and the PhNH fragment add across the borylene center and one of the silylene silicon atoms, respectively.[56] These observations, together with the broad small-molecule activation chemistry of base-stabilized aryl borylenes, motivated us to investigate the potential of borylene species in the activation of amines and phosphines.

[a]*Institute for Inorganic Chemistry, Julius-Maximilians-Universität Würzburg, Am Hubland, 97074 Würzburg, Germany. E-mail: h.braunschweig@uni-wuerzburg.de*

[b]*Institute for Sustainable Chemistry & Catalysis with Boron, Julius-Maximilians-Universität Würzburg, Am Hubland, 97074 Würzburg, Germany*

† These authors contributed equally.

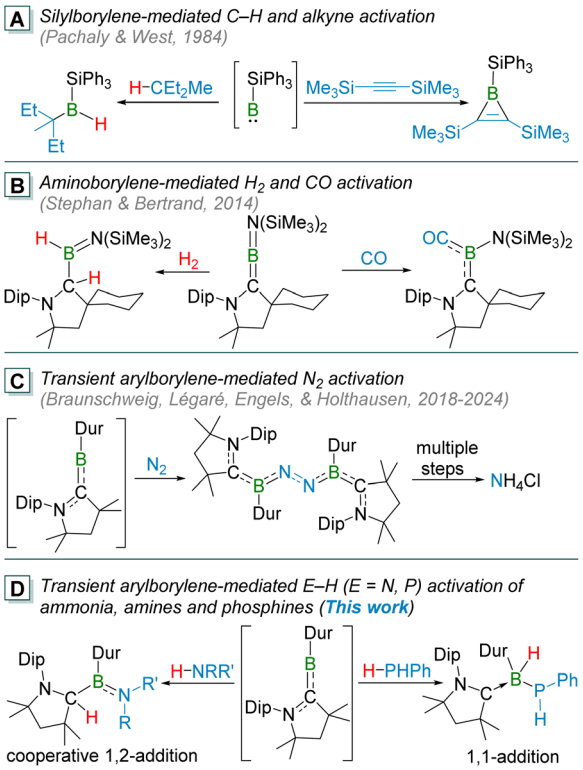

Fig. 1 Examples of borylene-mediated activation of various small molecules. Dur = 2,3,5,6-tetramethylphenyl; Dip = 2,6-diisopropylphenyl.

In this work, we present the cooperative 1,2-addition of N–H bonds from ammonia as well as primary and secondary amines across the C=B double bond of a transient CAAC-stabilized aryl borylene. In contrast, a similar reaction with a primary phosphine proceeds *via* 1,1-addition of the P–H bond at the borylene boron center.

Results and discussion

The transient dicoordinate borylene [(CAAC)BDur] (**3**) is generated *in situ* either by direct two-electron reduction of [(CAAC)BDurCl$_2$] (**1**) or through a stepwise reduction pathway involving the boryl radical intermediate [(CAAC)BDurCl]$^{\bullet}$ (**2**) (Scheme 1).[51,57]

The reduction of **1** with excess KC_8 (10 equiv.) in toluene under an overpressure of NH_3 (3 bar) afforded a colorless solid **4** in 90% yield (Scheme 1). The ^{11}B NMR spectroscopic resonance at $\delta = 45.8$ ppm, together with other spectroscopic data clearly identified compound **4** as the aminoborane [(CAACH)(Dur)B(NH$_2$)], which had previously been isolated as an intermediate during the conversion of the bis(borylene)–dinitrogen complex to ammonium chloride.[55] A singlet at $\delta = 4.08$ ppm in the ^{1}H NMR spectrum and a resonance at $\delta = 68.4$ ppm in the ^{13}C{^{1}H} NMR spectrum of **4** correspond to the migrated hydrogen atom and its host (formerly carbene) carbon atom, respectively.

Given the strongly reducing conditions employed for the *in situ* generation of [(CAAC)BDur], the possible *in situ* formation of potassium amide species was considered. To evaluate this possibility, a control experiment was performed in which [(CAAC)BDurCl$_2$] was treated independently with a potassium amide under similar conditions. However, no formation of compound **4** was observed. Instead, the reaction afforded unidentified product(s), as indicated by a single ^{11}B NMR resonance at $\delta = 30.7$ ppm. This suggests that potassium amide is unlikely to be responsible for the formation of **4** under the reaction conditions shown in Scheme 1.

To gain insight into the driving force governing the formation of aminoborane **4**, we carried out a detailed computational study on the reaction of transient borylene **3** with NH_3 (Fig. 2), which revealed a feasible two-step mechanism. In the first step, the amine lone pair interacts with the vacant p orbital of the borylene boron to form the borylene–NH_3 adduct $\mathbf{4}^{\mathbf{Int}}$, a highly exergonic process ($\Delta G^{\circ}_{\mathrm{Int}} = -24.6$ kcal mol^{-1}) consistent with the high accepting ability of the borylene boron, as indicated by the low-lying LUMO ($E_{\pi^*} = 0.34$ eV) and the positive natural charge at boron ($q_B = +0.87$) of **3**. In the second step, the boron-centered lone pair of the adduct $\mathbf{4}^{\mathbf{Int}}$ polarizes one N–H bond, generating $H^{\delta+}$ and $NH_2^{\delta-}$ fragments, as revealed by the natural charge on the NH_2 nitrogen atom and the H atom in the transition state ($\mathbf{4}^{\mathbf{TS}}$) (Fig. 2 and Table S1). The $H^{\delta+}$ migrates to the electron-rich carbene carbon of the CAAC ligand (Table S1), while the $NH_2^{\delta-}$ fragment forms a multiple bond with boron, affording the 1,2-addition product aminoborane **4**. The high energy barrier for this step ($\Delta G^{\circ}_{\mathrm{TS}} = 36.3$ kcal mol^{-1}) accounts for the requirement of elevated NH_3 pressure in the synthesis of **4**. The formation of **4** is further driven by the pronounced exergonicity of the overall reaction ($\Delta G^{\circ}_{\mathrm{Total}} = -57.9$ kcal mol^{-1}). Notably, a 1,1-addition pathway is not feasible, likely due to the electron deficiency at boron of adduct $\mathbf{4}^{\mathbf{Int}}$ ($q_B = +0.53$). These computational results, together with a previous theoretical

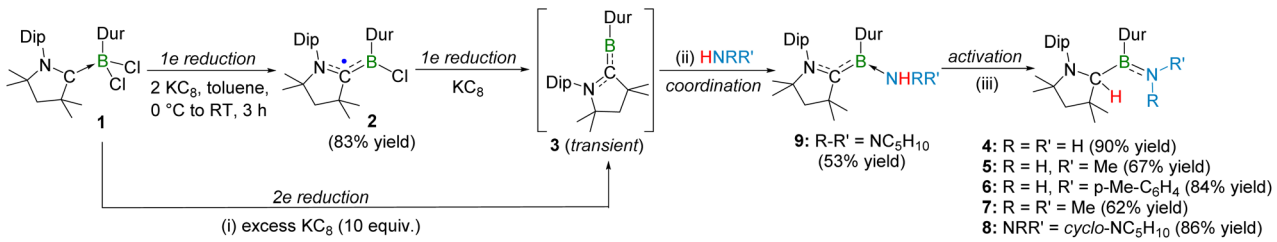

Scheme 1 General scheme for the borylene-mediated coordination and N–H activation of ammonia, primary and secondary amines. (i) −90 °C, toluene (for the synthesis of **4**, **5**, **7**, and **9**); −100 °C, Et$_2$O (for the synthesis of **6**). (ii) NH_3 (3 bar), −90 °C to RT, 1 h (for **4**); NH_2Me (3 bar), −90 °C to RT, 3 h (for **5**); *p*-toluidine (2 equiv.), −100 °C to RT, 3 h (for **6**); NMe_2 (1 bar), −90 °C to RT, 3 h (for **7**); piperidine (2 equiv.), −90 °C to RT, 2 h (for **9**). (iii) 80 °C, 16 h (for the synthesis of **8** from **9**).

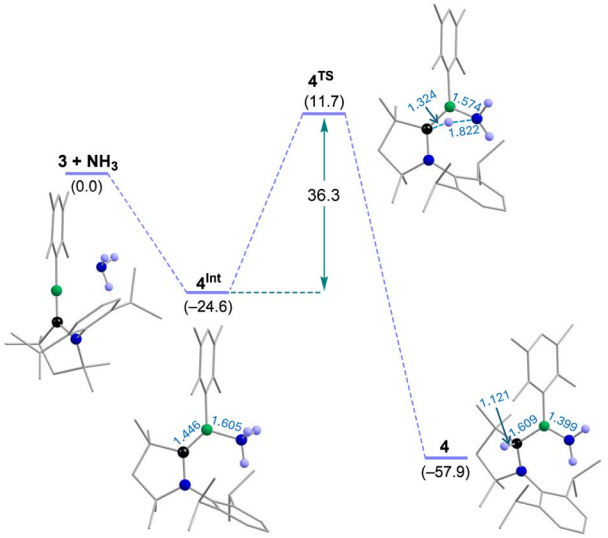

Fig. 2 Calculated reaction profile diagram illustrating the activation of NH_3 by transient borylene **3**. The reaction free energies and bond lengths are given in kcal mol^{-1} and Å, respectively. All hydrogen atoms, except those of the ammonia fragment, are omitted for clarity.

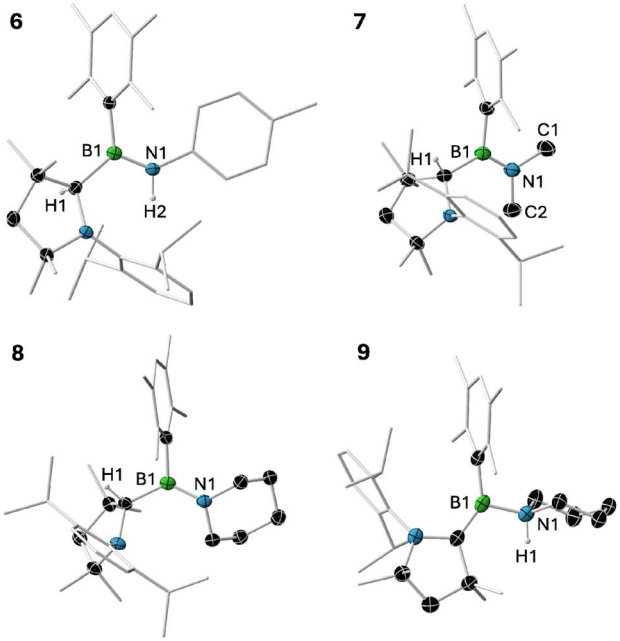

Fig. 3 Crystallographically-determined molecular structures of **6**–**9** (ellipsoids shown at the 50% probability level). All hydrogen atoms except those attached to the NBC^{CAAC} core, and the ellipsoids of the ligand periphery, are omitted for clarity.

study on various dicoordinate borylenes by Phukan and us,[58] suggest that this reactivity can be extended to higher amines.

The reaction of **1** with excess KC_8 (10 equiv.) and primary amines, namely methylamine (3 bar) or *para*-toluidine, yielded colourless solid **5** (67% yield) and light red solid **6** (84% yield), respectively (Scheme 1). The ^{11}B NMR spectra of **5** and **6** showed broad resonances at $\delta = 44.4$ and 44.8 ppm, respectively, slightly upfield shifted compared to that of aminoborane **4**. Also, the ^1H NMR spectra of **5** and **6** showed singlets at $\delta = 4.03$ and 4.18 ppm, respectively, similar to the signal for the C_{CAAC}–*H* nucleus of aminoborane **4**. The $^{13}C\{^1H\}$ NMR spectra of **5** and **6** showed chemical shifts at $\delta = 68.6$ and 69.3 ppm, respectively, which are slightly downfield compared to the signal corresponding to the former carbene carbon center (the carbon atom bearing the migrated hydrogen) in aminoborane **4**. These data collectively indicate borylene-mediated N–H bond cleavage of the primary amines and formation of aminoboranes, confirmed by single-crystal X-ray diffraction (SCXRD) analyses. The SCXRD studies revealed compounds **5** and **6** as aminoboranes [(CAACH)(Dur)B(NHMe)] and [(CAACH)(Dur)B(NH(*p*-Tol))], respectively (Fig. S30 and 3). The B–N bond distance in aminoborane **6** (1.402(2) Å) is marginally longer than that of aminoborane **4** (1.376(2) Å), yet comparable to that of aminoborane [(*t*Bu)(C_6F_5)BN(B(C_6F_5)$_2$)(*t*Bu)][59] (1.392(2) Å), indicative of partial double-bond character. The HOMO−5 of **5** (Fig. 4) and HOMO−1 of **6** (Fig. 4) display clear π-bonding interactions between boron (B1) and nitrogen (N1), further supported by the calculated Mayer bond orders (MBOs: 1.54 (**5**), 1.47 (**6**)) and Wiberg bond indices (WBIs: 1.50 (**5**), 1.42 (**6**)). From ammonia to primary amines, an increase in steric bulk leads to a slight elongation of the B–N partial double bond, as evidenced by the calculated WBIs and MBOs (Table S2).

Likewise, reduction of **1** with excess KC_8 in the presence of the secondary amine dimethylamine led to N–H bond cleavage, generating aminoborane **7** in 62% yield (Scheme 1). The ^{11}B NMR ($\delta = 45.7$ ppm), ^1H NMR ($\delta = 3.75$ ppm for C_{CAAC}–*H*) and $^{13}C\{^1H\}$ NMR ($\delta = 73.3$ ppm for C_{CAAC}–H) spectra of **7** showed patterns similar to those of aminoboranes **4**–**6**. These spectroscopic similarities, together with SCXRD study (Fig. 3) confirmed the 1,2-N–H addition of dimethylamine to the C=B double bond of transient arylborylene **3**. The B–N bond distance of aminoborane **7** (1.3931(17) Å) is comparable with that of aminoborane **6**, suggesting its partial double-bond character. Furthermore, the HOMO−5 (Fig. 4), together with the calculated MBO (1.46) and WBI (1.48), supports the presence of a multiple-bonding interaction between boron (B1) and nitrogen (N1) in **7**.

Interestingly, reduction of **1** with excess KC_8 (10 equiv.) in the presence of the cyclic secondary amine, piperidine, afforded an orange solid **9** in 53% yield (Scheme 1). The ^{11}B NMR spectrum showed a resonance at $\delta = 24.7$ ppm, significantly upfield shifted compared to those of aminoboranes **4**–**7**. Notably, unlike aminoboranes **4**–**7**, no characteristic chemical shifts for the C_{CAAC}–H moiety were observed within $\delta = 3.75$–4.18 ppm region in the ^1H NMR spectrum and within $\delta = 68.4$–73.3 ppm region in the $^{13}C\{^1H\}$ NMR spectrum of **9**. An unambiguous explanation eluded us until a SCXRD study revealed compound **9** as a Werner-type CAAC-stabilized durylborylene–piperidine complex, [(CAAC)(Dur)B(Pip)] (Pip = piperidine) (Fig. 3). The B–N distance in **9** (1.608(2) Å) is significantly longer than those in aminoboranes **4**–**7**, lying instead within the typical range for B–N dative bonds (1.565(7)–1.771(3) Å).[60–62]

Upon heating a solid sample of durylborylene–piperidyl adduct **9** at 80 °C for 16 h, a colorless solid **8** was obtained in 86% yield (Scheme 1). The ^{11}B NMR resonance of **8** at $\delta =$

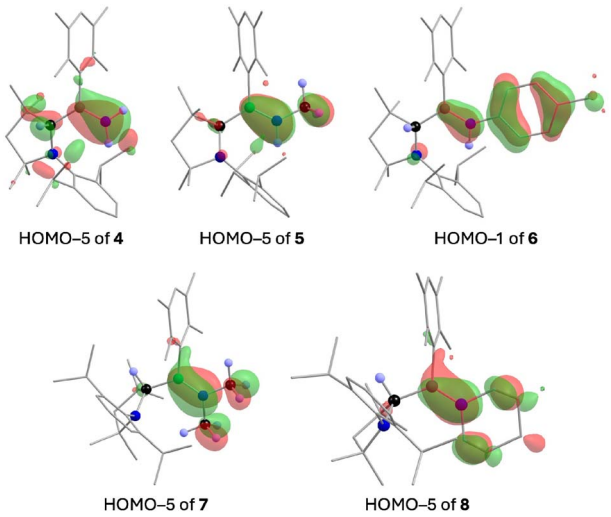

Fig. 4 Selected frontier molecular orbitals of **4–8** (isovalue 0.043 au), calculated at ωB97X-D/Def2-SVP level of theory.

44.4 ppm is comparable to those of aminoboranes **4–7**, indicating formation of the corresponding piperidine analogue. A singlet at $\delta = 3.81$ ppm in the ^{1}H NMR spectrum and a chemical shift at $\delta = 73.5$ ppm in the $^{13}C\{^{1}H\}$ NMR spectrum for C_{CAAC}–H moiety further support the identity of **8** as an aminoborane. SCXRD analysis confirmed the structure of **8** as aminoborane [(CAACH)(Dur)B(NPip)] (Fig. 3). The B–N bond distance in **8** (1.3944(17) Å) is comparable to those in aminoboranes **6** and **7**. As in aminoboranes **4–7**, the HOMO−5 of **8** showed a distinct π-bonding interaction between boron (B1) and nitrogen (N1) (Fig. 4). The calculated MBO (1.48) and WBI (1.50) for the B1–N1 bond **8** are comparable to those of aminoborane **7**. The isolation of the Werner-type durylborylene–piperidine coordination complex **9** during the synthesis of aminoborane **8** is consistent with our proposed borylene-mediated adduct formation, followed by 1,2-N–H addition pathway (Fig. 2). It is noteworthy that aminoboranes **4–8** showed ^{15}N chemical shifts in the range of $\delta = -246$ to -282 ppm for the nitrogen atom involved in the B=N double bond, whereas the single-bonded nitrogen atom of the CAACH ligand shows ^{15}N chemical shifts in the range of $\delta = -314$ to -326 ppm. These observations suggest that participation of the nitrogen lone pair in π-bonding with boron reduces the local electron density at nitrogen relative to a purely single-bonded nitrogen environment.

We then extended our studies to primary and secondary phosphines, heavier group 15 species with weaker E–H bonds, in order to investigate the prospect of the formation of a Werner-type borylene–phosphine adduct or P–H activation products. Our group recently reported that the use of tertiary phosphine PMe_3 enabled the isolation of borylene–phosphine adducts.[63–65] Herein, we studied the reactivity of borylene **3** with primary and secondary phosphines. The reduction of CAAC-stabilized durylboryl radical **2** with excess KC_8 (10 equiv.) in the presence of a primary phosphine, phenylphosphine, afforded an orange solid **10** in 80% yield (Scheme 2). Note that compound **10** can also be isolated from the reaction of adduct **1** with excess KC_8 (10 equiv.) in the presence of phenylphosphine under the same conditions; however, the yield is significantly lower. Unlike aminoboranes **4–8**, the ^{11}B NMR spectrum of **10** showed a high-field doublet of doublets at $\delta = -16.3$ ppm, coupled to both proton ($^{2}J_{B-H} = 84$ Hz) and phosphorus ($^{2}J_{B-P} = 24$ Hz). Moreover, no characteristic chemical shifts for the C_{CAAC}–*H* moiety were found in the ^{1}H and $^{13}C\{^{1}H\}$ NMR spectra of **10**, ruling out its possibility of being a 1,2-P–H addition product. Instead, a broad ^{1}H chemical shift at $\delta = 3.5$ ppm was observed, suggesting the presence of a B–H unit. Further, the $^{31}P\{^{1}H\}$ NMR spectrum showed a signal at $\delta = -91.9$ ppm. Collectively, these spectroscopic features indicate a 1,1-addition of the P–H bond across the boron center of the transient borylene **3**. Indeed, the SCXRD study confirmed compound **10** as [(CAAC)BH(Dur)(PHPh)] (Scheme 2), a product of 1,1-P–H-bond addition of phenylphosphine to the boron center of the transient durylborylene **3**. The B–P bond distance in **10** (2.015(1) Å) is slightly longer than the B–P single covalent bond (1.974(2) Å) in $[(Me_3P)(C_6H_4CH_2PCy_2)BrB_2(PHPh)]$,[66] but slightly shorter than that in $[(PPh_2)B_2H(C_6H_4CH_2PCy_2)_2]$ (2.051(2) Å).[66] Furthermore, the WBI and MBO of 0.99 and 0.95, respectively, corroborate a single bonding interaction between B1 and P1 in **10**.

It is noteworthy that, unlike the 1,2-N–H addition observed for amines, the reaction with phenylphosphine afforded a 1,1-P–H addition product, likely due to the lower electronegativity of phosphorus compared to nitrogen. Therefore, we investigated the possible reaction mechanism for P–H activation of

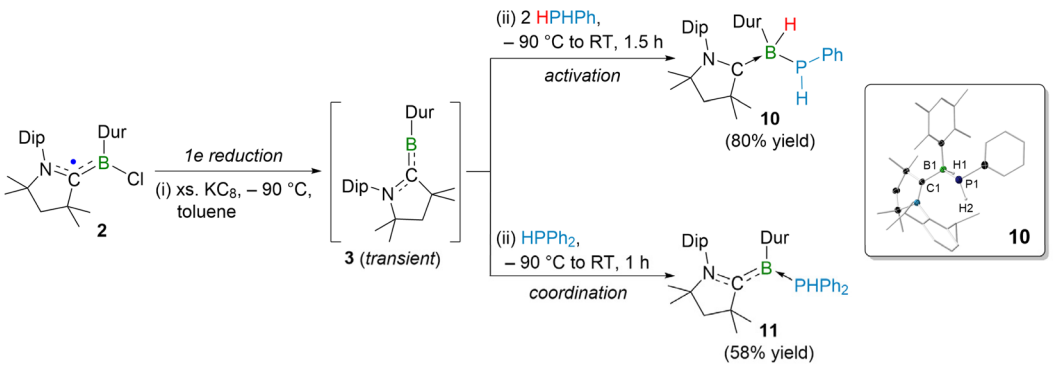

Scheme 2 Synthesis of borylene-mediated P–H activated (**10**) and coordinated (**11**) species. xs. = 10 equiv. (for the synthesis of **10**) and 8 equiv. (for the synthesis of **11**). Inset: Crystallographically-determined molecular structure of **10** (ellipsoids shown at the 50% probability level). All hydrogen atoms and ellipsoids of ligand periphery are omitted for clarity.

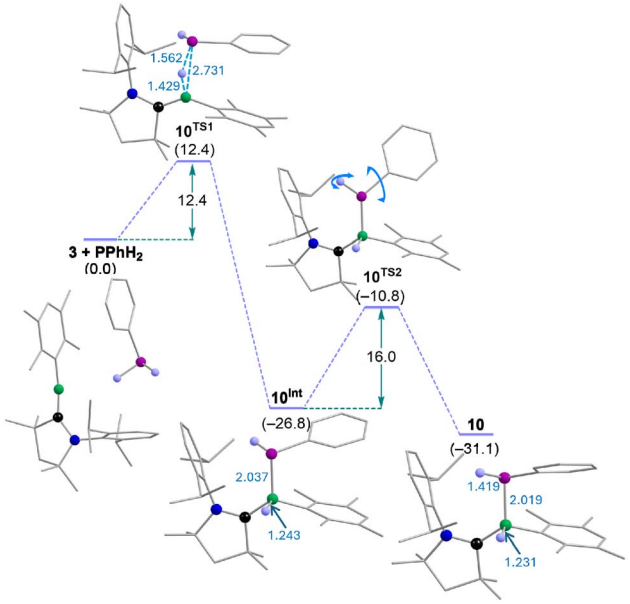

Fig. 5 Reaction profile diagram illustrating the activation of $PPhH_2$ by transient borylene **3**. The reaction free energies and bond lengths are given in kcal mol^{-1} and Å, respectively. All hydrogen atoms of ligand periphery are omitted for clarity.

phenylphosphine by the transient borylene **3** (Fig. 5). In the first step, the boron-centered lone pair of borylene **3** interacts with a P–H bond, forming a three-membered B···P···H ring in the transition state (**10^{TS1}**), probably due to the comparable electronegativity of P and H. In **10^{TS1}**, the P–H bond is slightly polarized (Table S1). Thereafter, cleavage of the P–H bond results in migration of the slightly positive PPhH fragment to the filled orbital of boron, while the hydrogen atom transfers to the vacant orbital of boron, affording the 1,1-P–H addition product **10^{Int}** (Fig. 5). In the second step, **10^{Int}** isomerizes to the thermodynamically stable product **10** *via* rotation of the phenyl group about the P–Ph bond and translation of the hydrogen atom of the P–H unit (Fig. 5). The free energy barriers associated with the formation of **10** (ΔG°_{TS1} = 12.4 kcal mol^{-1}, ΔG°_{TS2} = 16.0 kcal mol^{-1}) are relatively low, consistent with the mild experimental conditions. Another possible reaction mechanism for the formation of **10** involving the Werner-type adduct as an intermediate is less favorable, as it was calculated to have a significantly higher energy barrier for the 1,1-P–H activation step, which is inconsistent with the experimental reaction conditions.

On the other hand, the reaction of CAAC-stabilized durylboryl radical **2** with excess KC_8 (8 equiv.) and a secondary phosphine, diphenylphosphine, afforded an orange solid (**11**) in 58% yield. Interestingly, the ^{11}B NMR spectrum of **11** showed an intense chemical shift at δ = 0.7 ppm, appearing in the region characteristic of CAAC/phosphine-stabilized borylenes, suggesting the formation of a borylene–diphenylphosphine adduct.[63–65] Although SCXRD data obtained for **11** was of poor quality, they provided sufficient evidence to confidently assign the compound as a borylene–diphenylphosphane adduct. Adduct **11** is thermally sensitive and decomposes upon heating to multiple unidentified products. However, unlike in the case of amines, no P–H activation was observed.

Conclusions

In summary, we have demonstrated the ability of transient CAAC-stabilized arylborylenes to activate N–H and P–H bonds of ammonia, amines and phosphines. The borylene engages in 1,2-addition with ammonia and various amines to afford a family of aminoboranes, while reactions with primary phosphines proceed *via* 1,1-addition at the boron center to yield phosphinoboranes. Computational studies revealed that these divergent reactivities stem from the interplay between boron's ambiphilicity and the substrate's electronegativity, with the 1,2-addition pathway favored for N–H activation and the 1,1-addition pathway for P–H activation. The isolation of a Werner-type intermediate in the amine system further corroborates a stepwise adduct-assisted mechanism. These findings collectively underscore the potential of borylenes as powerful, metal-free reagents for bond activation and functionalization chemistry. The presented study broadens the scope of main-group reactivity, hinting at potentially sustainable future alternatives to transition-metal-mediated transformations.

Author contributions

Supervision, funding acquisition, conceptualization: H. B.; conceptualization, formal analysis, investigation: M. W.; conceptualization, investigation, formal analysis, writing – original draft: S. K.; investigation, formal analysis: P. J.; writing – review & editing: R. D. D.

Conflicts of interest

There are no conflicts to declare.

Data availability

The data supporting this article have been included as part of the supplementary information (SI). Supplementary information: synthetic, spectroscopic, X-ray crystallographic and computational details. See DOI: https://doi.org/10.1039/d6sc00526h.

CCDC 2521121–2521126 contain the supplementary crystallographic data for this paper.[67a–f]

Acknowledgements

Financial support from the Deutsche Forschungsgemeinschaft is gratefully acknowledged (BR1149/22-2 and 466954611). S. K. thanks the Alexander von Humboldt Foundation for a postdoctoral fellowship.

Notes and references

1 S. Streiff and F. Jérôme, Hydroamination of Non-Activated Alkenes with Ammonia: A Holy Grail in Catalysis, *Chem. Soc. Rev.*, 2021, **50**, 1512–1521.
2 E. Vitaku, D. T. Smith and J. T. Njardarson, Analysis of the Structural Diversity, Substitution Patterns, and Frequency of Nitrogen Heterocycles among U.S. FDA Approved Pharmaceuticals, *J. Med. Chem.*, 2014, **57**, 10257–10274.
3 J. L. Klinkenberg and J. F. Hartwig, Catalytic Organometallic Reactions of Ammonia, *Angew. Chem., Int. Ed.*, 2011, **50**, 86–95.
4 H. Kim and S. Chang, The Use of Ammonia as an Ultimate Amino Source in the Transition Metal-Catalyzed C–H Amination, *Acc. Chem. Res.*, 2017, **50**, 482–486.
5 T. Irrgang and R. Kempe, Transition-Metal-Catalyzed Reductive Amination Employing Hydrogen, *Chem. Rev.*, 2020, **120**, 9583–9674.
6 D. F. McMillen and D. M. Golden, Hydrocarbon Bond-Dissociation Energies, *Ann. Rev. Phys. Chem.*, 1982, **33**, 493–532.
7 J. I. van der Vlugt, Advances in Selective Activation and Application of Ammonia in Homogeneous Catalysis, *Chem. Soc. Rev.*, 2010, **39**, 2302–2322.
8 A. L. Casalnuovo, J. C. Calabrese and D. Milstein, N-H Activation. 1. Oxidative Addition of Ammonia to Iridium(I). Isolation, Structural Characterization, and Reactivity of Amidoiridium Hydrides, *Inorg. Chem.*, 1987, **26**, 971–973.
9 J. Zhao, A. S. Goldman and J. F. Hartwig, Oxidative Addition of Ammonia to Form a Stable Monomeric Amido Hydride Complex, *Science*, 2005, **307**, 1080–1082.
10 E. Morgan, D. F. MacLean, R. McDonald and L. Turculet, Rhodium and Iridium Amido Complexes Supported by Silyl Pincer Ligation: Ammonia N–H Bond Activation by a [PSiP]Ir Complex, *J. Am. Chem. Soc.*, 2009, **131**, 14234–14236.
11 E. Khaskin, M. A. Iron, L. J. W. Shimon, J. Zhang and D. Milstein, N–H Activation of Amines and Ammonia by Ru via Metal–Ligand Cooperation, *J. Am. Chem. Soc.*, 2010, **132**, 8542–8543.
12 D. V. Gutsulyak, W. E. Piers, J. Borau-Garcia and M. Parvez, Activation of Water, Ammonia, and Other Small Molecules by $PC_{carbene}P$ Nickel Pincer Complexes, *J. Am. Chem. Soc.*, 2013, **135**, 11776–11779.
13 Y. H. Chang, Y. Nakajima, H. Tanaka, K. Yoshizawa and F. Ozawa, Facile N–H Bond Cleavage of Ammonia by an Iridium Complex Bearing a Noninnocent PNP-Pincer Type Phosphaalkene Ligand, *J. Am. Chem. Soc.*, 2013, **135**, 11791–11794.
14 R. M. Brown, J. B. Garcia, J. Valjus, C. J. Roberts, H. M. Tuononen, M. Parvez and R. Roesler, Ammonia Activation by a Nickel NCN-Pincer Complex featuring a Non-Innocent N-Heterocyclic Carbene: Ammine and Amido Complexes in Equilibrium, *Angew. Chem., Int. Ed.*, 2015, **54**, 6274–6277.
15 G. L. Hillhouse and J. E. Bercaw, Reactions of Water and Ammonia with Bis(pentamethylcyclopentadienyl) Complexes of Zirconium and Hafnium, *J. Am. Chem. Soc.*, 1984, **106**, 5472–5478.
16 G. W. Margulieux, M. J. Bezdek, Z. R. Turner and P. J. Chirik, Ammonia Activation, H_2 Evolution and Nitride Formation from a Molybdenum Complex with a Chemically and Redox Noninnocent Ligand, *J. Am. Chem. Soc.*, 2017, **139**, 6110–6113.
17 C. M. Fafard, D. Adhikari, B. M. Foxman, D. J. Mindiola and O. V. Ozerov, Addition of Ammonia, Water, and Dihydrogen across a Single Pd–Pd Bond, *J. Am. Chem. Soc.*, 2007, **129**, 10318–10319.
18 F. Alonso, I. P. Beletskaya and M. Yus, Transition-Metal-Catalyzed Addition of Heteroatom–Hydrogen Bonds to Alkynes, *Chem. Rev.*, 2004, **104**, 3079–3160.
19 T. E. Müller, K. C. Hultzsch, M. Yus, F. Foubelo and M. Tada, Hydroamination: Direct Addition of Amines to Alkenes and Alkynes, *Chem. Rev.*, 2008, **108**, 3795–3892.
20 S. Ma and J. F. Hartwig, Progression of Hydroamination Catalyzed by Late Transition-Metal Complexes from Activated to Unactivated Alkenes, *Acc. Chem. Res.*, 2023, **56**, 1565–1577.
21 M. Kosugi, M. Kameyama and T. Migita, Palladium-catalyzed Aromatic Amination of Aryl Bromides with n,n-Di-Ethylamino-tributyltin, *Chem. Lett.*, 1983, **12**, 927–928.
22 F. Paul, J. Patt and J. F. Hartwig, Palladium-catalyzed formation of carbon-nitrogen bonds. Reaction intermediates and catalyst improvements in the hetero cross-coupling of aryl halides and tin amides, *J. Am. Chem. Soc.*, 1994, **116**, 5969–5970.
23 A. S. Guram and S. L. Buchwald, Palladium-Catalyzed Aromatic Aminations with in situ Generated Aminostannanes, *J. Am. Chem. Soc.*, 1994, **116**, 7901–7902.
24 P. A. Forero-Cortés and A. M. Haydl, The 25th Anniversary of the Buchwald–Hartwig Amination: Development, Applications, and Outlook, *Org. Process Res. Dev.*, 2019, **23**, 1478–1483.
25 G. D. Frey, V. Lavallo, B. Donnadieu, W. W. Schoeller and G. Bertrand, Facile Splitting of Hydrogen and Ammonia by Nucleophilic Activation at a Single Carbon Center, *Science*, 2007, **316**, 439–441.
26 Y. Peng, B. D. Ellis, X. Wang and P. P. Power, Diarylstannylene Activation of Hydrogen or Ammonia with Arene Elimination, *J. Am. Chem. Soc.*, 2008, **130**, 12268–12269.
27 Z. Zhu, X. Wang, Y. Peng, H. Lei, J. C. Fettinger, E. Rivard and P. P. Power, Addition of Hydrogen or Ammonia to a Low-Valent Group 13 Metal Species at 25 °C and 1 atm, *Angew. Chem., Int. Ed.*, 2009, **48**, 2031–2034.
28 A. Jana, C. Schulzke and H. W. Roesky, Oxidative Addition of Ammonia at a Silicon(II) Center and an Unprecedented Hydrogenation Reaction of Compounds with Low-Valent Group 14 Elements Using Ammonia Borane, *J. Am. Chem. Soc.*, 2009, **131**, 4600–4601.
29 J. A. B. Abdalla, I. M. Riddlestone, R. Tirfoin and S. Aldridge, Cooperative Bond Activation and Catalytic Reduction of

Carbon Dioxide at a Group 13 Metal Center, *Angew. Chem., Int. Ed.*, 2015, **54**, 5098–5102.

30 A. V. Protchenko, J. I. Bates, L. M. A. Saleh, M. P. Blake, A. D. Schwarz, E. L. Kolychev, A. L. Thompson, C. Jones, P. Mountford and S. Aldridge, Enabling and Probing Oxidative Addition and Reductive Elimination at a Group 14 Metal Center: Cleavage and Functionalization of E–H Bonds by a Bis(Boryl)Stannylene, *J. Am. Chem. Soc.*, 2016, **138**, 4555–4564.

31 D. Wendel, T. Szilvási, D. Henschel, P. J. Altmann, C. Jandl, S. Inoue and B. Rieger, Precise Activation of Ammonia and Carbon Dioxide by an Iminodisilene, *Angew. Chem., Int. Ed.*, 2018, **57**, 14575–14579.

32 A. L. Humphries, G. A. Tellier, M. D. Smith, A. R. Chianese and D. V. Peryshkov, N-H Bond Activation of Ammonia by a Redox-Active Carboranyl Diphosphine, *J. Am. Chem. Soc.*, 2024, **146**, 33159–33168.

33 S. M. McCarthy, Y.-C. Lin, D. Devarajan, J. W. Chang, H. P. Yennawar, R. M. Rioux, D. H. Ess and A. T. Radosevich, Intermolecular N–H Oxidative Addition of Ammonia, Alkylamines, and Arylamines to a Planar σ^3-Phosphorus Compound via an Entropy-Controlled Electrophilic Mechanism, *J. Am. Chem. Soc.*, 2014, **136**, 4640–4650.

34 J. Cui, Y. Li, R. Ganguly, A. Inthirarajah, H. Hirao and R. Kinjo, Metal-Free σ-Bond Metathesis in Ammonia Activation by a Diazadiphosphapentalene, *J. Am. Chem. Soc.*, 2014, **136**, 16764–16767.

35 T. P. Robinson, D. M. De Rosa, S. Aldridge and J. M. Goicoechea, E–H Bond Activation of Ammonia and Water by a Geometrically Constrained Phosphorus(III) Compound, *Angew. Chem., Int. Ed.*, 2015, **54**, 13758–13763.

36 J. Abbenseth, O. P. E. Townrow and J. M. Goicoechea, Thermoneutral N–H Bond Activation of Ammonia by a Geometrically Constrained Phosphine, *Angew. Chem., Int. Ed.*, 2021, **60**, 23625–23629.

37 S. Volodarsky and R. Dobrovetsky, Ambiphilic Geometrically Constrained Phosphenium Cation, *Chem. Commun.*, 2018, **54**, 6931–6934.

38 F. Dankert, J.-E. Siewert, P. Gupta, F. Weigend and C. Hering-Junghans, Metal-Free N–H Bond Activation by Phospha-Wittig Reagents, *Angew. Chem., Int. Ed.*, 2022, **61**, e202207064.

39 P. L. Timms, Boron-Fluorine Chemistry. I. Boron Monofluoride and Some Derivatives, *J. Am. Chem. Soc.*, 1967, **89**, 1629–1632.

40 S. Aldridge and D. L. Coombs, Transition metal boryl and borylene complexes: substitution and abstraction chemistry, *Coord. Chem. Rev.*, 2004, **248**, 535–559.

41 H. Braunschweig, R. D. Dewhurst and V. H. Gessner, Transition metal borylene complexes, *Chem. Soc. Rev.*, 2013, **42**, 3197–3208.

42 D. W. Stephan, A Tale of Two Elements: The Lewis Acidity/Basicity Umpolung of Boron and Phosphorus, *Angew. Chem., Int. Ed.*, 2017, **56**, 5984–5992.

43 M. Soleilhavoup and G. Bertrand, Borylenes: An Emerging Class of Compounds, *Angew. Chem., Int. Ed.*, 2017, **56**, 10282–10292.

44 M.-A. Légaré, C. Pranckevicius and H. Braunschweig, Metallomimetic Chemistry of Boron, *Chem. Rev.*, 2019, **119**, 8231–8261.

45 L. Andrews, P. Hassanzadeh, J. M. L. Martin and P. R. Taylor, Pulsed laser evaporated boron atom reactions with acetylene. Infrared spectra and quantum chemical structure and frequency calculations for several novel organoborane BC_2H_2 and HBC_2 molecules, *J. Phys. Chem.*, 1993, **97**, 5839–5847.

46 H. F. Bettinger, Phenylborylene: Direct Spectroscopic Characterization in Inert Gas Matrices, *J. Am. Chem. Soc.*, 2006, **128**, 2534–2535.

47 K. Edel, M. Krieg, D. Grote and H. F. Bettinger, Photoreactions of Phenylborylene with Dinitrogen and Carbon Monoxide, *J. Am. Chem. Soc.*, 2017, **139**, 15151–15159.

48 B. Pachaly and R. West, Photochemical Generation of Triphenylsilylboranediyl $(C_6H_5)_3SiB$: From Organosilylboranes, *Angew. Chem., Int. Ed.*, 1984, **23**, 454–455.

49 R. Kinjo, B. Donnadieu, M. A. Celik, G. Frenking and G. Bertrand, Synthesis and characterization of a neutral tricoordinate organoboron isoelectronic with amines, *Science*, 2011, **333**, 610–613.

50 F. Dahcheh, D. Martin, D. W. Stephan and G. Bertrand, Synthesis and Reactivity of a CAAC–Aminoborylene Adduct: A Hetero-Allene or an Organoboron Isoelectronic with Singlet Carbenes, *Angew. Chem., Int. Ed.*, 2014, **53**, 13159–13163.

51 M.-A. Légaré, G. Bélanger-Chabot, R. D. Dewhurst, E. Welz, I. Krummenacher, B. Engels and H. Braunschweig, Nitrogen fixation and reduction at boron, *Science*, 2018, **359**, 896–900.

52 M.-A. Légaré, M. Rang, G. Bélanger-Chabot, J. I. Schweizer, I. Krummenacher, R. Bertermann, M. Arrowsmith, M. C. Holthausen and H. Braunschweig, The reductive coupling of dinitrogen, *Science*, 2019, **363**, 1329–1332.

53 A. Gärtner, U. S. Karaca, M. Rang, M. Heinz, P. D. Engel, I. Krummenacher, M. Arrowsmith, A. Hermann, A. Matler, A. Rempel, R. Witte, H. Braunschweig, M. C. Holthausen and M.-A. Légaré, Achieving Control over the Reduction/Coupling Dichotomy of N_2 by Boron Metallomimetics, *J. Am. Chem. Soc.*, 2023, **145**, 8231–8241.

54 M. Weber, T. Kupfer, M. Arrowsmith, R. D. Dewhurst, M. Rang, B. Ritschel, S. Titlbach, M. Ernst, M. O. Rodrigues, E. N. da Silva Júnior and H. Braunschweig, Bypassing Ammonia: From N_2 to Nitrogen Heterocycles without N1 Intermediates or Transition Metals, *Angew. Chem., Int. Ed.*, 2024, **63**, e202402777.

55 M.-A. Légaré, G. Bélanger-Chabot, M. Rang, R. D. Dewhurst, I. Krummenacher, R. Bertermann and H. Braunschweig, One-pot, room-temperature conversion of dinitrogen to

ammonium chloride at a main-group element, *Nat. Chem.*, 2020, **12**, 1076–1080.

56 X. Chen, Y. Yang, H. Wang and Z. Mo, Cooperative Bond Activation and Catalytic CO_2 Functionalization with a Geometrically Constrained Bis(silylene)-Stabilized Borylene, *J. Am. Chem. Soc.*, 2023, **145**, 7011–7020.

57 P. Bissinger, H. Braunschweig, A. Damme, I. Krummenacher, A. K. Phukan, K. Radacki and S. Sugawara, Isolation of a Neutral Boron-Containing Radical Stabilized by a Cyclic (Alkyl)(Amino)Carbene, *Angew. Chem., Int. Ed.*, 2014, **53**, 7360–7363.

58 B. Chakraborty, F. E. Basumatary, H. Braunschweig and A. K. Phukan, Cooperative Activation of Small Molecules by Base-Stabilized Borylenes, *Inorg. Chem.*, 2023, **62**, 9063–9076.

59 L. Winner, G. Bélanger-Chabot, M. A. Celik, M. Schäfer and H. Braunschweig, Intriguing migrations in transient iminoborane adducts: two new pathways to aminoboranes, *Chem. Commun.*, 2018, **54**, 9349–9351.

60 R. Boese, N. Niederprüm and D. Bläser, The boron-nitrogen bond. Structural investigations, in *Molecules in Natural Science and Medicine*, ed. Z. B. Maksic, M. Eckert-Masic and E. Horwood, Chichester, England, 1992.

61 W. T. Klooster, T. F. Koetzle, P. E. M. Siegbahn, T. B. Richardson and R. H. Crabtree, Study of the N-H···H-B Dihydrogen Bond Including the Crystal Structure of BH_3NH_3 by Neutron Diffraction, *J. Am. Chem. Soc.*, 1999, **121**, 6337–6343.

62 K. Chernichenko, M. Nieger, M. Leskelä and T. Repo, Hydrogen activation by 2-boryl-*N*,*N*-dialkylanilines: a revision of Piers' *ansa*-aminoborane, *Dalton Trans.*, 2012, **41**, 9029–9032.

63 C. Pranckevicius, C. Herok, F. Fantuzzi, B. Engels and H. Braunschweig, Bond-Strengthening Backdonation in Aminoborylene-Stabilized Aminoborylenes: At the Intersection of Borylenes and Diborenes, *Angew. Chem., Int. Ed.*, 2019, **58**, 12893–12897.

64 M. Arrowsmith, S. Endres, M. Heinz, V. Nestler, M. C. Holthausen and H. Braunschweig, Probing the Boundaries between Lewis-Basic and Redox Behavior of a Parent Borylene, *Chem.–Eur. J.*, 2021, **27**, 17660–17668.

65 M. Michel, L. Endres, F. Fantuzzi, I. Krummenacher and H. Braunschweig, Harnessing transient CAAC-stabilized mesitylborylenes for chalcogen activation, *Chem. Sci.*, 2025, **16**, 5632–5639.

66 T. E. Stennett, A. Jayaraman, T. Brückner, L. Schneider and H. Braunschweig, Hydrophosphination of boron-boron multiple bonds, *Chem. Sci.*, 2020, **11**, 1335–1341.

67 (*a*) CCDC 2521121: Experimental Crystal Structure Determination, 2026, DOI: 10.5517/ccdc.csd.cc2qmfh9; (*b*) CCDC 2521122: Experimental Crystal Structure Determination, 2026, DOI: 10.5517/ccdc.csd.cc2qmfjb; (*c*) CCDC 2521123: Experimental Crystal Structure Determination, 2026, DOI: 10.5517/ccdc.csd.cc2qmfkc; (*d*) CCDC 2521124: Experimental Crystal Structure Determination, 2026, DOI: 10.5517/ccdc.csd.cc2qmfld; (*e*) CCDC 2521125: Experimental Crystal Structure Determination, 2026, DOI: 10.5517/ccdc.csd.cc2qmfmf; (*f*) CCDC 2521126: Experimental Crystal Structure Determination, 2026, DOI: 10.5517/ccdc.csd.cc2qmfng.